scientific reports

Check for updates

OPEN

Magnetism and magnetoresistance in the critical region of a dilute ferromagnet

M. Wang✉, B. Howells, R. A. Marshall, J. M. Taylor, K. W. Edmonds, A. W. Rushforth, R. P. Campion & B. L. Gallagher

We present detailed experimental measurements and simulations of the field-dependent magnetization and magnetoresistance in the vicinity of the Curie temperature in the highly disordered dilute ferromagnetic semiconductor (Ga,Mn)As. The observed dependence of the magnetization on external magnetic field and temperature is consistent with three-dimensional Heisenberg equation of state calculations including a narrow distribution of critical temperatures. The magnetoresistance shows a peak at the Curie temperature due to the suppression of magnetic scattering in an applied magnetic field, which is well-described by considering changes in the square of the magnetization induced by the magnetic field.

The critical behavior of ferromagnetic materials around their Curie temperature (T_C) is of fundamental interest. Close to T_C, magnetic properties such as magnetization and magnetic susceptibility are determined by critical fluctuations and show power-law behavior[1]. The electrical resistivity and the magnetization are closely related, with short-range magnetization fluctuations giving rise to a temperature-dependence of the resistivity and resulting in a resistive anomaly at T_C[2]. In addition, in ferromagnets the electrical resistivity tensor is dependent on the orientation of the magnetization, giving rise to longitudinal and transverse anisotropic magnetoresistance (AMR) effects[3].

Dilute ferromagnetic semiconductors, in which a few percent transition metal ions are substituted into a non-magnetic matrix, represent a model strongly disordered system[4]. In particular, (Ga,Mn)As has been widely studied as a testbed for studies of spintronics and magnetoresistance phenomena[5–8]. The Mn dopant is an acceptor when it substitutes for Ga, providing both localized magnetic moments and delocalized holes. The ferromagnetism in (Ga,Mn)As is due to the interaction between the magnetic moments and holes. More recent studies have identified a wide range of dilute ferromagnetic semiconductor systems with independent carrier and spin doping[9,10].

Studies of critical behavior of the magnetization in dilute ferromagnetic semiconductors have produced disparate and contradictory results[11–15] (see Ref.[16] for a detailed discussion). In a previous study[16], we obtained the critical exponents in the highly disordered dilute ferromagnetic semiconductor (Ga,Mn)As by fitting of Kouvel–Fisher[17] plots within the region around 2.5% > $|t|$ > 0.5%, where $t = (T − T_C)/T_C$ is the reduced temperature. The accessible range of t is limited by the strong intrinsic disorder as well as large lengthscale inhomogeneity. Here we extend this study by considering also the field-dependence of magnetization and magnetoresistance in the critical region. While the close connection between magnetization and electrical resistance is very well established[18], critical magnetoresistance has been little-studied in dilute ferromagnetic semiconductors[19]. The increase of magnetic susceptibility around T_C leads to an increased ordering of magnetic moments and decreased charge carrier scattering which manifests itself as a negative magnetoresistance (MR). Thus, the magnetoresistance should behave critically around T_C[20–23].

Results

The study was performed on samples cut from a 25 nm (Ga,Mn)As layer with 12% nominal Mn concentration, grown by low temperature molecular beam epitaxy (MBE) on a GaAs(001) substrate[24]. The sample was annealed at 180 °C, resulting in a measured $T_C = (183.5 ± 0.1)$ K as obtained from a Kouvel–Fisher plot[16]. Due to small differences in the fluxes and substrate temperature between the center and edge of the wafer, there was a small and approximately linear variation of T_C across the sample[16]. The sample had uniaxial anisotropy with easy axis along the [1$\bar{1}$0] crystal direction[25].

School of Physics and Astronomy, University of Nottingham, University Park, Nottingham NG7 2RD, UK. ✉email: mu.wang@nottingham.ac.uk
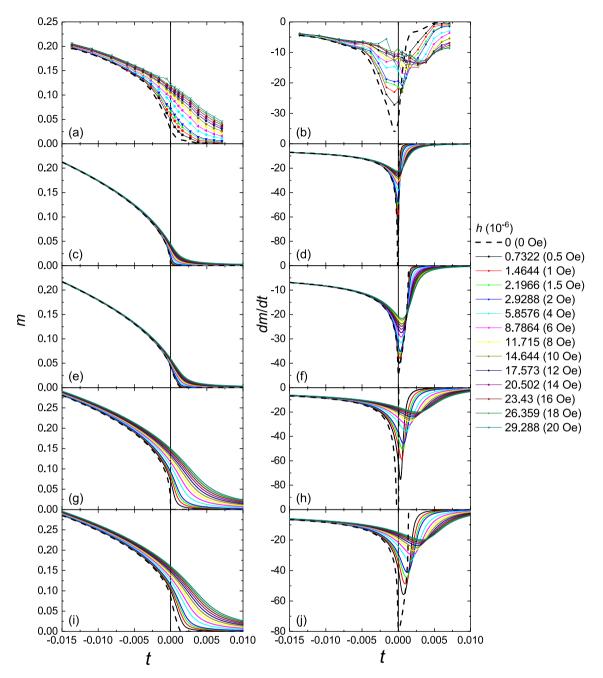
nature portfolio

Figure 1. *m* vs. *t* and *dm/dt* vs. *t* plots for different applied magnetic fields. (**a**, **b**) Experimental result obtained by SQUID magnetometry for a 25 nm (Ga,Mn)As film. (**c**, **d**) Calculation using the mean field equation of state for a uniform sample. (**e**, **f**) Calculation using the mean field equation of state with 0.5 K T_C broadening. (**g**, **h**) Calculation using the 3D Heisenberg equation of state for a uniform sample. (**i**, **j**) Calculation using the 3D Heisenberg equation of state with 0.5 K T_C broadening.

Magnetization and its temperature derivative. Detailed magnetometry measurements around the Curie temperature were performed on a 4-mm-sized sample. The sample was first field cooled to 2 K to form a single domain state with saturation magnetization (M_s) of 65 emu/cm^3. To compare with the simulation result, the magnetometry data are presented in dimensionless quantities of reduced magnetization $m = M/M_s$, reduced magnetic field $h = \mu_0 \mu_B H / k_B T_C$ and reduced temperature t. Here μ_0 is the vacuum permeability, μ_B is the Bohr magneton, and k_B is the Boltzmann constant.

Figure 1a shows the temperature-dependent reduced magnetization (m vs. t) curves with external magnetic field up to 20 Oe applied along the magnetic easy axis. The magnetization does not drop to zero sharply but has a tail around T_C. The size of the tail is field-dependent and can extend more than 1% t (~ 2 K) above the real T_C when only a few Oe field is applied. Figure 1b shows the temperature derivative of m (dm/dt vs. t) calculated by numerical differentiation. The dm/dt vs. t curve has a sharp minimum around T_C. The peak becomes broader and moves to the right as the magnetic field increases (up to 0.4% of t, for $H = 20$ Oe).

Within the critical region, the relation of m, h, and t can be described by an approximate equation of state for the limit of small t, m, and h/m[26]:

$$\left(\frac{h}{m}\right)^{1/\gamma} = at + bm^{1/\beta}$$

with model-dependent critical exponents β, γ and amplitudes a, b. We first performed the numerical simulation to obtain the m vs. t curves around T_C using the mean field model with critical exponents $\beta = 0.5$, $\gamma = 1$ and amplitudes $a = 1$, $b = 1/3$ for the simulation. We also introduced a rectangular distribution for T_C of 0.5 K (0.28% or ±0.14% of T_C) to simulate a sample with a linear variation of T_C from one side to the other. The calculations (Fig. 1c–f) indicate a much weaker effect of the external magnetic field compared to the experimental result. For a uniform sample, no shift in the minimum of the simulated dm/dt is observed as the field increases (Fig. 1d). Even with the inclusion of the 0.5 K T_C broadening, the dm/dt minimum still only shifts by a maximum of 0.05% (Fig. 1f). Hence, the critical behavior of the highly disordered (Ga,Mn)As system is not well described by the mean field equation of state.

Using three-dimensional Heisenberg critical exponents ($\beta = 0.369$, $\gamma = 1.396$) and amplitudes ($a = 0.82$, $b = 0.4$), the simulated m vs. t curves show similar shape, size and field-dependence of the tail when compared with the experimental data (Fig. 1g–j). The shift of the minimum of dm/dt with increasing field is also quantitatively consistent with the experiment. These results indicate that the field- and temperature-dependence of the magnetization in the critical region is well-described by the three-dimensional Heisenberg model.

Magnetoresistance. Magnetoresistance measurements were conducted on two 285 μm × 45 μm Hall bars with current channels along the easy [1$\bar{1}$0] and hard [110] crystalline axes, respectively. The devices were initially field-cooled from room temperature to 2 K to form a single domain state. Then, the longitudinal resistance (R_{xx}) was measured in zero field as the temperature was increased to above 200 K (Fig. 2a). The Curie temperatures of 178.8 ± 0.2 K and 176.1 ± 0.2 K were estimated from the peak positions in the temperature derivative of the resistivity curves[27]. The reduction of T_C compared to the magnetometry sample is because the devices were fabricated from different part of the wafer, and possibly also due to the effect of photolithography and etching.

Magnetoresistance measurements were performed at temperatures around T_C with up to 15 Oe field applied along the [1$\bar{1}$0] crystal direction (Fig. 2b,c). The magnetoresistance is defined as the change of resistance when applying a magnetic field:

$$MR = \frac{R_{xx}(H) - R_{xx}(0)}{R_{xx}(0)}$$

where $R_{xx}(H)$ is the longitudinal resistance in an applied magnetic field of strength H. As temperature approaches T_C from below, the MR becomes more and more negative. The MR then becomes less negative with a modified shape of the MR curve after the temperature rises above T_C. The most negative MR curve corresponds to a temperature which is slightly higher than the T_C obtained from the peak in the temperature derivative of the resistivity. Small differences are observed between the two devices.

We distinguish between anisotropic magnetoresistance (AMR), due to the dependence on the direction of the magnetization relative to the current and crystal, and isotropic MR, which below we relate to the suppression of magnetization fluctuations by the magnetic field. To remove the AMR contribution, we take the average of the $|MR|$ for the [1$\bar{1}$0] and [110] oriented Hall bars at each reduced temperature t (temperature normalized using Curie temperatures obtained previously) where the external magnetic field is respectively parallel and perpendicular to the current.

Figure 3a,b show the resulting $|MR|$ as well as $|MR|/H$ versus reduced temperature for different values of H. The curves show a clear peak at $t = 0$, which broadens and shifts slightly to higher temperatures with increasing magnetic field. The peak is particularly pronounced for the $|MR|/H$ curves, with a full width at half maximum of around 0.5% (1 K) for the lowest magnetic fields used.
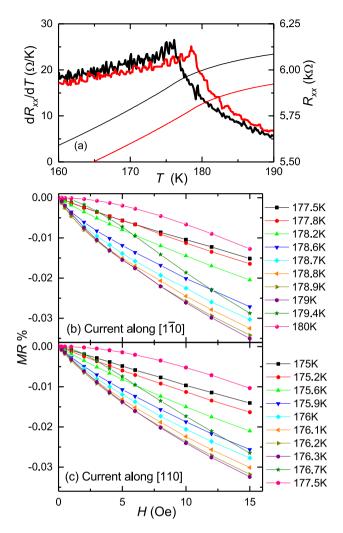
Magnetization fluctuations in a ferromagnet close to T_C result in a contribution to the electrical resistivity, which in the lowest order approximation is proportional to $[1 - m(H,T)^2]$[18,20–23]. Hence, the relationship between the magnetoresistance and the magnetization in the critical region can be described as:
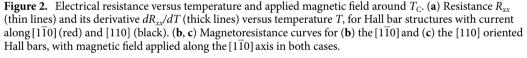
$$|MR| \propto \left(m^2\right)$$

where $\left(m^2\right) = m^2(h) - m^2(0)$. Figure 3c,d show the plots of $\delta(m^2)$ and $\delta(m^2)/h$ vs. t, obtained from the magnetometry data. Similar to the magnetoresistance behavior, the curves are sharply peaked at $t = 0$, with a crossover of the $\delta(m^2)/h$ curves at $t > 0$. Simulated curves using the three-dimensional Heisenberg equation of state (Fig. 3e–h) are consistent with both the magnetoresistance and magnetometry experimental results. They also show a clear effect of inhomogeneity, with significant broadening and shift of the peak when a 0.5 K rectangular broadening of T_C is included.

Discussion

Our results demonstrate that the magnetoresistance in the critical region of (Ga,Mn)As is well-described by considering only the magnetic field-induced suppression of magnetization fluctuations. The very sharp cusp of MR/H, due to its dependence on the square of the magnetization at a given magnetic field, provides a unique probe of the ferromagnetic phase transition. It can be used for accurate determination of T_C, which is an important benchmark property of dilute ferromagnetic semiconductors[5,9,10,19,24,27,28].

Figure 2. Electrical resistance versus temperature and applied magnetic field around T_C. (**a**) Resistance R_{xx} (thin lines) and its derivative dR_{xx}/dT (thick lines) versus temperature T, for Hall bar structures with current along [1$\bar{1}$0] (red) and [110] (black). (**b**, **c**) Magnetoresistance curves for (**b**) the [1$\bar{1}$0] and (**c**) the [110] oriented Hall bars, with magnetic field applied along the [1$\bar{1}$0] axis in both cases.

Calculations using an approximate equation of state with three-dimensional Heisenberg-like critical exponents are in good agreement with the measured magnetic field-dependent magnetization in the critical region, and by extension also with the magnetoresistance. In contrast, mean-field critical exponents give a substantial reduction of the field-induced magnetization at temperatures around T_C, compared to the measured data. The mean-field model underestimates the suppression of magnetization fluctuations by an applied magnetic field around T_C[29]. As a result, the mean-field calculated field-dependence of the peak position of dm/dt is rather weak.

The observed agreement of field-dependent magnetization of (Ga,Mn)As in the critical region around T_C is well-described by calculations with the 3D Heisenberg model. This is consistent with our previous study of the thermoremanent magnetization in a similar set of samples, for which 3D Heisenberg-like critical exponents were obtained using Kouvel–Fisher analysis[16]. However, due to the intrinsic disorder present in randomly substituted dilute ferromagnetic semiconductors such as (Ga,Mn)As, the accessible critical region is limited to reduced temperatures $|t| < 0.025$. Any long-range inhomogeneities in the samples will further limit the critical region and may be responsible for some apparently contradictory results in earlier studies[11–15]. Hence, the observed good agreement of the field-induced magnetization with the three-dimensional Heisenberg model, as shown in Fig. 1, provides an important validation of the results of Ref.[16]. This does not rule out the possibility that other universality classes may be found by tailoring the properties of the material, for example by inducing a strong uniaxial magnetic anisotropy by growth on relaxed (In,Ga)As buffer[30]. The dependence of T_C (x) in (Ga$_{1-x}$,Mn$_x$) As (shown in e.g. Ref.[24]) points to a long-range character of the spin–spin interactions.

The magnetization and magnetoresistance measurements and calculations further demonstrate the marked effect of even a moderate broadening of $\Delta T_C = 0.5$ K $= \pm 0.14$%. The peak in the calculated $\delta(m^2)/h$ becomes broader and shifts to higher temperature when the broadening is included. The effect of broadening due to inhomogeneity can also be observed in the experimental magnetoresistance traces; for example, the largest $|MR|$ is observed at a higher temperature than the T_C estimated from the dR_{xx}/dT curves.
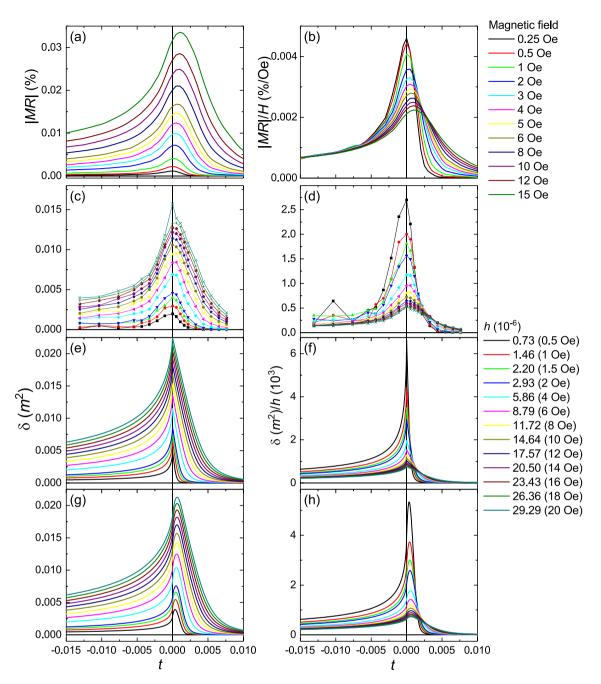
Figure 3. Magnetoresistance and $\delta(m^2) = m^2(h) - m^2(0)$ vs. reduced temperature at different applied magnetic fields. (**a**, **b**) Measured $|MR|$ and $|MR|/H$ vs. t for the (Ga,Mn)As Hall bars. Measurements for currents along $[1\bar{1}0]$ and $[110]$ have been averaged to remove the anisotropic magnetoresistance. (**c**, **d**) $\delta(m^2)$ vs. t and $\delta(m^2)/h$ vs. t calculated from the magnetometry measurements shown in Fig. 1. (**e**, **f**) Numerical simulation of $\delta(m^2)$ vs. t and $\delta(m^2)/h$ vs. t using the three-dimensional Heisenberg model for a uniform sample. (**g**, **h**) Simulation including T_C broadening of 0.5 K.

Methods

Sample preparation. A 25 nm of (Ga,Mn)As with 12% nominal Mn concentration was grown on a 2 in. GaAs(001) wafer at 200 °C by molecular beam epitaxy. The sample was annealed at 180 °C for 48 h to remove the interstitial Mn. Hall bars with current channel width of 45 μm, and voltage probes separated by 285 μm, were fabricated by standard photolithography with 20 nm Ti/100 nm Au contact pads for four terminal transport measurements.

Magnetometry measurement. The 4-mm-sized sample was measured using a Quantum design MPMS system. The sample first has been measured at 2 K to obtain the saturation magnetization. Then the system has been carefully demagnetized to reduce the remanent field within magnet coil to less than 0.5 Oe, before performing the detailed measurements around Curie temperature.

Magnetotransport measurement. 4 terminal DC transport measurements were performed in an Oxford Instruments cryostat system. A Keithley 2400 Sourcemeter was used for applying 0.1 mA constant current along the Hall bars and a Keithley 2000 Multimeter was used for measuring the longitudinal voltages. The cryostat sample space and electromagnetic coil were covered by a mu-metal cylinder to provide magnetic shielding. The remanent field within the sample space is less than 0.1 Oe measured by a calibrated Hall probe.

Numerical simulation. The numerical simulation was coded in Python language. Newton–Raphson method was used to find the magnetization values giving roots of the equations of state at each temperature and magnetic field.

References

1. Binney, J. J., Dowrick, N. J., Fisher, A. J. & Newman, M. E. J. *The Theory of Critical Phenomena* (Oxford Science Publications, Oxford, 1992).
2. Fisher, M. E. & Langer, J. S. Resistive anomalies at magnetic critical points. *Phys. Rev. Lett.* **20**, 665–668 (1968).
3. McGuire, T. & Potter, R. Anisotropic magnetoresistance in ferromagnetic 3d alloys. *IEEE Trans. Magn.* **11**, 1018–1038 (1975).
4. Priour, D. J. & Das Sarma, S. Critical behavior of diluted magnetic semiconductors: Apparent violation and eventual restoration of the Harris criterion for all regimes of disorder. *Phys. Rev. B* **81**, 224403 (2010).
5. Ohno, H. Making nonmagnetic semiconductors ferromagnetic. *Science* **281**, 951–956 (1998).
6. Dietl, T. & Ohno, H. Dilute ferromagnetic semiconductors: physics and spintronic structures. *Rev. Mod. Phys.* **86**, 187–251 (2014).
7. Jungwirth, T. *et al.* Spin-dependent phenomena and device concepts explored in (Ga, Mn)As. *Rev. Mod. Phys.* **86**, 855–896 (2014).
8. Rushforth, A. W. *et al.* Anisotropic magnetoresistance components in (Ga, Mn)As. *Phys. Rev. Lett.* **99**, 147207 (2007).
9. Deng, Z. *et al.* Li(Zn, Mn)As as a new generation ferromagnet based on a I–II–V semiconductor. *Nat. Commun.* **2**, 422 (2011).
10. Zhao, K. *et al.* New diluted ferromagnetic semiconductor with Curie temperature up to 180 K and isostructural to the '122' iron-based superconductors. *Nat. Commun.* **4**, 1442 (2013).
11. Jiang, W. *et al.* Critical behavior from the anomalous Hall effect in (GaMn)As. *Phys. Rev. B* **80**, 214409 (2009).
12. Khazen, Kh. *et al.* Intrinsically limited critical temperatures of highly doped $Ga_{1−x}Mn_xAs$ thin films. *Phys. Rev. B* **81**, 235201 (2010).
13. Yuldashev, S. U. *et al.* Study of $Ga_{1−x}Mn_xAs$ critical behavior by using thermal diffusivity. *J. Korean Phys. Soc.* **59**, 431 (2011).
14. Yuldashev, S. *et al.* Specific heat study of GaMnAs. *Appl. Phys. Express* **3**, 073005 (2010).
15. Stafanowicz, S. *et al.* Phase diagram and critical behavior of the random ferromagnet GaMnN. *Phys. Rev. B* **88**, 081201 (2013).
16. Wang, M. *et al.* Three-dimensional Heisenberg critical behavior in the highly disordered dilute ferromagnetic semiconductor (Ga, Mn)As. *Phys. Rev. B* **93**, 184417 (2016).
17. Kouvel, J. S. & Fisher, M. E. Detailed magnetic behavior of nickel near its Curie point. *Phys. Rev.* **136**, A1626 (1964).
18. Gerlach, W. & Englert, E. A new relation between electrical resistance and energy of magnetisation. *Nature* **128**, 151–152 (1931).
19. Kwiatkowski, A. *et al.* Determining Curie temperature of (Ga, Mn)As samples based on electrical transport measurements: Low Curie temperature case. *Appl. Phys. Lett.* **108**, 242103 (2016).
20. Schwerer, F. C. Magnetic field dependence of the electrical resistivity of nickel near its Curie temperature. *Phys. Rev. B* **9**, 958 (1974).
21. Balberg, I. & Helman, J. S. Critical behavior of the resistivity in magnetic systems. *Phys. Rev. B* **18**, 303 (1978).
22. Freitas, P. P. & Sousa, J. B. Critical behavior of the magnetoresistance of Gd near the Curie point: An experimental test of theoretical models. *J. Phys. F: Met. Phys.* **13**, 1245 (1983).
23. Dubowik, J., Zaleski, K., Goscianska, I., Glowinski, H. & Ehresmann, A. Magnetoresistance and its relation to magnetization in $Ni_{50}Mn_{35}Sn_{15}$ shape-memory epitaxial films. *Appl. Phys. Lett.* **100**, 162403 (2012).
24. Wang, M. *et al.* Obtaining high Curie temperatures in (Ga, Mn)As. *Appl. Phys. Lett.* **93**, 132103 (2008).
25. Sawicki, M. *et al.* In-plane uniaxial anisotropy rotations in (Ga, Mn)As. *Phys. Rev. B* **71**, 121302(R) (2005).
26. Arrott, A. & Noakes, J. E. Approximate equation of state for nickel near its Curie temperature. *Phys. Rev. Lett.* **19**, 786–789 (1967).
27. Novak, V. *et al.* Curie point singularity in the temperature derivative of resistivity in (Ga, Mn)As. *Phys. Rev. Lett.* **101**, 077201 (2008).
28. Wang, M. *et al.* Determining Curie temperatures in dilute ferromagnetic semiconductor: High Curie temperature (Ga, Mn)As. *Appl. Phys. Lett.* **104**, 132406 (2014).
29. Sliwa, C. & Dietl, T. Thermodynamic and thermoelectric properties of (Ga, Mn)As and related compounds. *Phys. Rev. B* **83**, 245210 (2011).
30. Yamanouchi, M., Chiba, D., Matsukura, F., Dietl, T. & Ohno, H. Velocity of domain-wall motion induced by electrical current in the ferromagnetic semiconductor (Ga, Mn)As. *Phys. Rev. Lett.* **96**, 096601 (2006).

Author contributions

M.W., K.W.E., A.W.R. and B.L.G. were responsible for the experimental design. R.P.C. performed the material growth. M.W., R.A.M. and A.W.R. performed the magnetometry measurements and analyzed the data. M.W. fabricated the devices. M.W., B.H. and J.M.T. performed the magneto-transport measurements and data analysis. M.W. and J.M.T. performed the numerical simulation. M.W. and K.W.E. wrote the manuscript with contributions from all authors.

Competing interests

The authors declare no competing interests.

Additional information

Correspondence and requests for materials should be addressed to M.W.

Reprints and permissions information is available at www.nature.com/reprints.

Publisher's note Springer Nature remains neutral with regard to jurisdictional claims in published maps and institutional affiliations.